

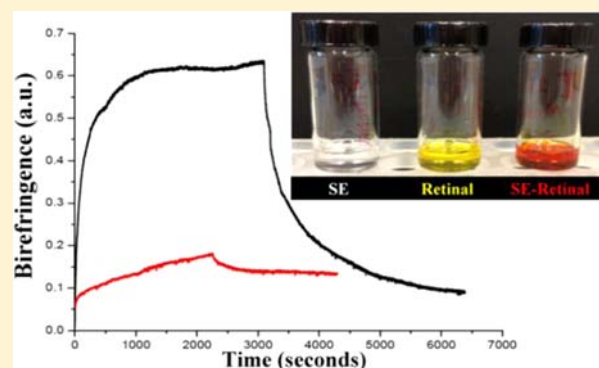
Photoresponsive Retinal-Modified Silk–Elastin Copolymer

Zhongyuan Sun, Guokui Qin, Xiaoxia Xia, Mark Cronin-Golomb, Fiorenzo G. Omenetto, and David L. Kaplan*

Department of Biomedical Engineering, 4 Colby Street, Tufts University, Medford, Massachusetts 02155, United States

S Supporting Information

ABSTRACT: The chimeric proteins, silk–elastin-like protein polymers (SELPs), consist of repeating units of silk and elastin to retain the mechanical strength of silk, while incorporating the dynamic environmental sensitivity of elastin. A retinal-modified SELP was prepared, modified, and studied for photodynamic responses. The protein was designed, cloned, expressed, and purified with lysine present in the elastin repeats. The purified protein was then chemically modified with the biocompatible moiety retinal via the lysine side chains. Structural changes with the polymer were assessed before and after retinal modification using Fourier transform infrared spectroscopy and circular dichroism spectroscopy. Optical studies and spectral analysis were performed before and after retinal modification. The random-coil fraction of the protein increased after retinal modification while the β -sheet fraction significantly decreased. Birefringence of the modified protein was induced when irradiated with a linearly polarized 488 nm laser light. Retinal modification of this protein offers a useful strategy for potential use in biosensors, controlled drug delivery, and other areas of biomedical engineering.



INTRODUCTION

Protein-based biomaterials such as silks,¹ elastins,² collagens,^{3,4} and resilins⁵ are studied for drug delivery and tissue engineering because of their biocompatibility, controllable degradation and minimal cytotoxicity.⁶ Recombinant DNA technologies allow the synthesis of biopolymers with precise control of primary sequence and chain length, as well as placement of chemical handles to permit functionalization to enhance interactions with cells and surfaces. This versatility and control of protein polymers provides remarkable design options to extend biological and mechanical properties. Silk–elastin-like protein polymers (SELPs), consisting of repeating units of silk and elastin, have been utilized to exploit the mechanical strength of silk with the environmental sensitivity of elastin.⁷ Some SELPs have been fabricated into nanoparticles, hydrogels, micro-diameter fibers, and nanofibrous scaffolds, displaying useful properties for drug delivery and tissue engineering.^{3,7–14} The structure of SELPs can be modified at the single amino acid residue level to allow the introduction of functional motifs to control self-assembly and sensitivity to external stimuli.⁹ For example, in our previous studies, a two-step self-assembly process of SELPs was reported relative to the ratio of silk-to-elastin domains, indicating the potential tunable control of structural transitions.⁷

The small size of the repetitive sequence in the elastin primary structure, such as VPGXG (X = V, I, or A), allows for the introduction of alternative amino acid residues such as K, Y, and E for facile chemical modifications of the polypeptides.³ Azobenzene derivatives, a group of photosensitive molecules,

were successfully introduced onto genetically engineered elastin molecules, and the transition temperature (T_c) of these modified elastins was controlled by ultraviolet irradiation due to the *trans*–*cis* isomerization of the azobenzene groups.¹⁵ Azo-modified silk films, synthesized via diazonium coupling between tyrosine residues of silk and azobenzene derivatives, also demonstrated nonlinear optical properties, such as optically induced birefringence, holographic recording, and optically induced surface relief gratings.¹⁶ The studies of these materials related to optical holography, reaction efficiencies, and ultrafast dynamics are all areas of interest in the optics and materials communities. While azo materials do possess attractive optical properties, their questionable biocompatibility motivated us to consider the use of retinal, which as the basis of the visual system, represents a truly biocompatible photosensitizer. Retinal also has more complex photoisomerization pathways and so is more amenable to engineering optimization.

Retinal is a promising candidate for holographic memory applications triggered by all-*trans* to *cis* isomerization of a protein-bound retinal protonated Schiff base (RPSB) chromophore.^{17,18} Recently, new retinal nanoceramic thin films have been fabricated for photonic applications, and the Schiff base in the retinal films had a substantial effect on optical properties, suggesting a good candidate for holographic storage.¹⁸ In the present study, SELPs were synthesized and modified with retinal protonated Schiff Base, to generate a material for light-

Received: December 27, 2012

Published: February 5, 2013

induced dynamic changes. This new SELP, termed PS2E8K, includes the introduction of lysine. The structure and optical properties of the protein were analyzed by circular dichroism (CD) spectroscopy, Fourier transform infrared (FTIR) spectroscopy, and optical polarization.

RESULTS AND DISCUSSION

SELP Synthesis and Purification. Seamless cloning strategies were used for the biosynthesis of the SELP⁷ and PS2E8K with a silk-to-elastin ratio of 2:8 generated with lysine (K) in the second amino acid position of the fifth elastin block. This chemical handle provided for further chemical cross-linking via $-NH_2$ groups. The purity and molecular weight of the SELPs was confirmed by sodium dodecyl sulfate polyacrylamide gel electrophoresis (SDS-PAGE) analysis (Figure 1A). The yield of purified PS2E8K was about 50

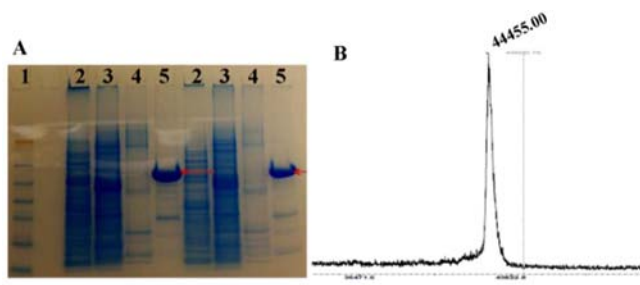


Figure 1. Characterization of purified SELP PS2E8K. (A) Protein purification determination by 4–12% SDS-PAGE: lane 1, Seeblue plus2 prestained standard (Invitrogen) used as size markers (188, 98, 62, 49, 38, 28, 17, 14, 6, 3 kDa); lanes 2–4, collected fractions from Ni–NTA columns after washing buffer; lane 5, collected fractions from Ni–NTA columns with elution buffer. (B) MALDI-TOF mass spectrum of PS2E8K.

mg/L. The molecular weight of PS2E8K was 38–49 kDa (Figure 1A), estimated from SDS-PAGE, and determined to be 44.5 kDa by matrix-assisted laser desorption time-of-flight mass spectrometry (MALDI-TOF MS) (Figure 1B).

Chemical Modification. The formation of a Schiff base between the lysine and retinal was conducted as shown in Figure 2. The amine groups of lysine side chains act as nucleophilic agents and attack the aldehyde carbons of retinal molecules to form carbon nitrogen double bonds under basic



Figure 2. Schematic for retinal modification of the lysine residues in the silk–elastin copolymer PS2E8K. Insert: chemical reactions for PS2E8K before and after retinal modification (left, PS2E8K in DMSO solution; middle, retinal molecules in DMSO solution; right, retinal-modified PS2E8K in DMSO solution).

environment. Once the photosensitive molecules were integrated into PS2E8Y, optical properties of the modified biopolymer were investigated (Figure 2). Organic solvents can induce β sheets to form with silk proteins and result in insolubility;^{1,5} therefore, we selected dimethyl sulfoxide (DMSO) versus methanol in these reactions to avoid this complication. The silk–elastin copolymer had good solubility in DMSO (Figure 2, insert). The retinal-modified silk–elastin products appear red-orange in color. This finding suggests that the retinal Schiff base was protonated and the positive charge delocalization along the conjugated carbon chain of retinal was stabilized by one or more interactions, such as hydrogen bonding or electrostatic repulsion, probably attributed from the appropriate folding of the copolymer. The charge delocalization caused redshifts of retinal-modified silk–elastin copolymer, but the hydrogen of the protonated Schiff base may not be distinguished by NMR spectra.^{17,19}

¹H NMR Analysis of SELPs before and after Retinal Modification. Comparative studies of SELPs before and after retinal modification were performed by ¹H NMR (Figure 3).

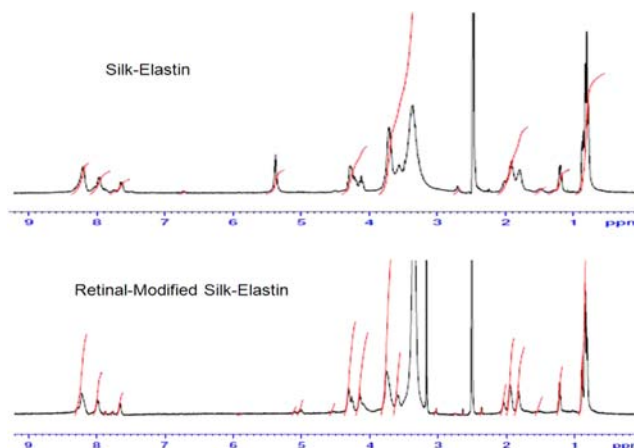


Figure 3. ¹H NMR analysis of SELPs before (upper panel) and after (lower panel) retinal modification.

SELP PS2E8K (500 MHz, DMSO-*d*₆): δ H/ppm 0.83, 0.89 (s, Val γ), 1.22, 1.23 (m, Ala β), 1.51 (br, Lys γ), 1.81 (br, Lys β /Lys δ), 1.90, 1.92 (br, Pro γ /Val β), 2.01 (m, Pro β), 3.57 (br, Pro δ), 3.72 (br, Ser β /Gly α), 4.12 (br, Gly α), 4.21 (br, Ala α /Val α /Lys α), 4.28 (br, Ser α /His α /Pro α), 7.63 (br, Lys ϵ (Lys–NH₂)), 7.98, 8.20 (br, HN/His δ , ϵ).

Retinal-modified SELP PS2E8K (500 MHz, DMSO-*d*₆): δ H/ppm 0.84, 0.89 (s, Val γ), 1.22, 1.23 (m, Ala β), 1.52 (br, Lys γ), 1.83 (br, Lys β /Lys δ), 1.95 (br, Pro γ /Val β), 2.04 (m, Pro β), 3.17 (s, His β), 3.60 (br, Pro δ), 3.75 (br, Ser β /Gly α), 4.15 (br, Gly α), 4.26 (br, Ala α /Val α /Lys α), 4.31 (br, Ser α /His α /Pro α), 7.65 (br, Lys ϵ (Lys–NH₂)), 7.98, 8.21 (br, HN/His δ , ϵ).

The chemical shift of Lys–NH₂ is around 7.65 ppm, and 3.57% of Lys–NH₂ dropped to 2.21% after retinal modification according to peak area integral analysis, implying that about 38.1% of lysine residues were involved in the Schiff base reaction. The peak of 2.51 ppm is assigned for DMSO-*d*₆ solvent, and 3.36 ppm is the peak of H₂O in CD₃SO.^{20,21}

Structural Characterization. Lyophilized powders or dried films of the recombinant protein and retinal-modified PS2E8K were examined by attenuated total reflectance (ATR) FTIR spectroscopy (Figure 4A), which includes an expansion of the amide I region for secondary structure analysis. The

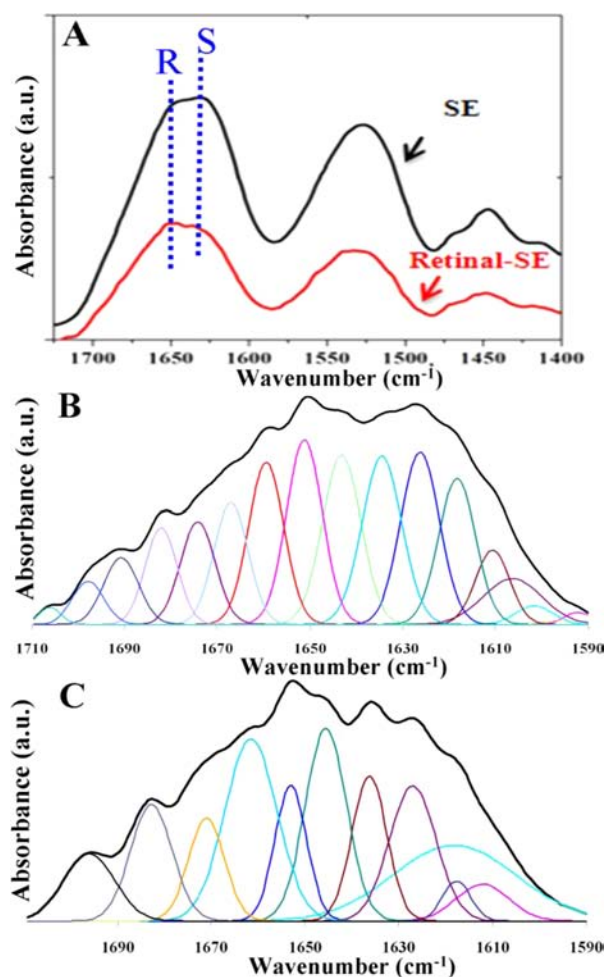


Figure 4. Structure characterization of unmodified and retinal-modified SELP PS2E8K by FTIR. (A) FTIR spectra: R represents random coil, S for β -sheet structure. (B, C) Selected FTIR absorbance spectra of unmodified (B) and retinal-modified (C) silk–elastin copolymer in the amide I' regions after Fourier self-deconvolution. The heavy line represents the deduced absorbance band. The light lines represent the contributions to the amide I' band.

broad nature of the amide I bands (centered around 1650 cm^{-1}) indicated a range of heterogeneous conformations for both the unmodified and retinal-modified silk–elastin copolymer PS2E8K. Peak deconvolution suggested potential contributions from all known secondary structures (Figure 4B,C). Secondary structure changes were further analyzed for the polymer PS2E8K before and after retinal modification (Table 1). Random coil content increased from 31% to 43% while the β -sheet content decreased from 31% to 20% before and after retinal modification, indicating that the modification induced conformational changes. To confirm the structural changes of the retinal-modified PS2E8K, secondary structure was also assessed by CD spectroscopy (Figure 5). CD spectra of both unmodified and retinal-modified PS2E8K showed an increase

Table 1. Secondary Structure of Unmodified and Retinal-Modified SELP PS2E8K by FTIR

	β sheet	random coil	α helix	turn
PS2E8K	31%	31%	13%	25%
retinal-modified PS2E8K	20%	43%	10%	26%

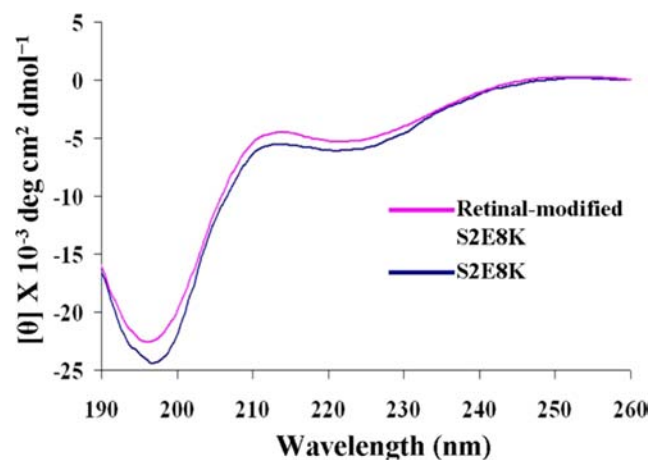


Figure 5. Far-UV CD spectra of unmodified and retinal-modified silk–elastin copolymer PS2E8K. All spectra were recorded at room temperature ($25\text{ }^{\circ}\text{C}$) using a 0.5 mm path length quartz cell with protein concentrations of 0.5 mg/mL .

in signal at 210 nm , suggestive of induction of a type II β -turn conformation, similar to elastin-like polymers as observed previously.⁷ The positive ellipticity at 190 nm and the negative ellipticity at 220 nm indicated the induction of a β -sheet conformation in both polymers, a feature usually observed for silk polymers.⁶ Compared with unmodified PS2E8K, the negative signal near 195 nm suggested more disordered structure in the retinal-modified PS2E8K, consistent with the FTIR spectra.

Optical Polarization and Spectral Analysis. Thin films of approximately $10\text{ }\mu\text{m}$ thick retinal-modified PS2E8K were prepared and dried on glass slides (Figure 6A). As reported previously and shown in Figure 6B,¹⁶ the probe was split into p and s polarization by means of a Wollaston prism after passing through the all-*trans* retinal-modified PS2E8K film. The setup was slightly different from that described in ref 15 in that the incident 632.8 nm probe beam was p polarized instead of circularly polarized. This change enabled more accurate measurement of the birefringence to be made, since the birefringence in the PS2E8k film was a factor of 10 lower than that observed for azo-modified silk. The smaller effect is more easily seen in an instrument where a null result leads to a zero output: p polarized light whose polarization is unaltered by the film is completely blocked by an orthogonally oriented polarizer. The intensity of the transmitted s polarized beams was monitored using photodiodes and compared to that resulting from the use of a known azo–silk standard. Figure 6C shows the birefringence versus exposure time of the all-*trans* retinal-modified silk–elastin copolymer when illuminated with 1 W cm^{-2} of 488 nm wavelength argon laser light. The first part of the figure is the response to linearly polarized light, and the second part is the erasure response to circularly polarized light. The retinal-modified films exhibited the optically induced effects similar to those found in other polymers incorporating azobenzene moieties, such as azobenzene modified *Bombyx mori* silk.¹⁶ We hypothesize that, initially, the all-*trans* retinal molecules retained their low energy state, the *trans* state. After the retinal-modified sample was irradiated by the light of proper wavelength with a polarization component parallel to the *trans* structure, the retinal molecule was excited to the *cis* state, while the excess *trans* isomers perpendicular to the polarization build up in a form of spatial hole burning. This optically induced

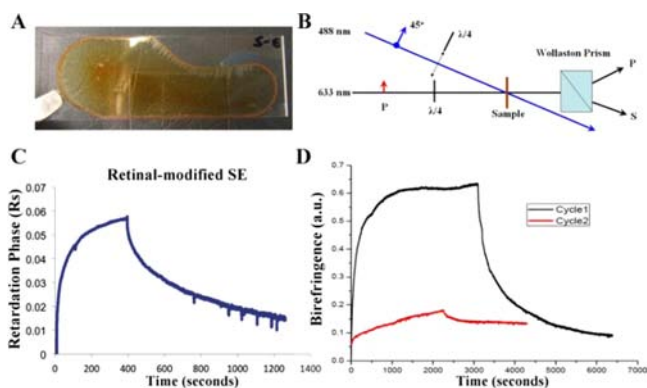


Figure 6. Optical polarization of retinal-modified polymer films. (A) Retinal-modified PS2E8K film dried onto a glass slide. (B) Birefringence measurement setup. The birefringence was written using a 488 nm argon ion laser beam polarized at 45° to the horizontal. The birefringence was probed with a p polarized He–Ne laser. In the absence of birefringence, the powers in the s polarization after the Wollaston prism was zero. In the presence of birefringence, the s polarized component became nonzero, and its magnitude indicated the extent of birefringence. The birefringence was erased by inserting a quarter-wave plate into the writing beam to render it circularly polarized. (C) Birefringence retardation versus exposure time of the retinal-modified silk–elastin copolymer PS2E8K, first with linearly polarized light to induce birefringence and then with circularly polarized light for erasure. The intensity of the actinic light was 1 W cm⁻² at a wavelength of 488 nm. (D) Birefringence retardation in PS2E8K for the same experimental conditions as C, showing the first cycle of recording and erasing and the second cycle in the same spot of recording and erasing. This behavior contrasts to that of azo–silk in which the second cycle would be the same as the first.

anisotropy in the all-*trans* retinal distribution leads to birefringence.¹⁶ Therefore, the detected birefringence of the retinal-modified silk–elastin copolymer was caused by the anisotropic structure of the sample that was induced by the *trans*–*cis* isomerization of retinal molecules. The double exponential data fits for birefringence retardation amplitude and time constants for azo–silk and retinal–PS2E8K are shown in Table 2.

Table 2. Double Exponential Data Fits for Azo–Silk and Retinal–PS2E8K

	steady-state phase retardation (rad)	time constant 1 (s)	time constant 2 (s)
azo–silk	1.38	6.2	173
retinal–PS2E8K	0.058	15.3	124

We also noticed that the optical behavior of retinal–silk–elastin was different from that of azo dye modified polymers. The optical effects in azo polymers are usually simply and repetitively reversible by switching the polarization of the incident light, since there is only one *cis* state,¹⁶ while the retinal molecule has several different *cis* states, such as 11-*cis*, 9-*cis*, and 13-*cis*. Retinal in the protein environment would give *trans* to 13-*cis* isomerization, while a retinal protonated Schiff base in solution would prefer *trans* to 11-*cis* transition,¹⁷ and which *cis* form generated in this situation needs to be determined in the near future work. After one cycle of writing and erasure, the optical sensitivity of the retinal-modified silk–elastin films was substantially reduced (Figure 6D).

Therefore, investigating the proportion of the various isomers in a retinal-modified silk–elastin film after light irradiation would be of interest, as well as detection of volume changes due to isomerization.^{22–24}

In total, the studies reported here demonstrate that this new SELP with retinal modifications provides a useful platform to study optically indicated changes in material structure and morphology.^{25,26} The tunable features of the proteins, the SELPs, combined with the interesting polarization associated changes in the structure, suggest future directions toward novel biomaterials for a range of potential utilities.^{27,28} This may include selective control of multimodal drug delivery, medical materials that can change properties upon irradiation inputs, and many related themes.

CONCLUSIONS

A recombinant SELP, PS2E8K, was generated and characterized as a soluble protein, with the lysine residues as chemical handles for reaction with retinal. The material features of both the unmodified and retinal-modified PS2E8K were investigated for structural and optical properties. The findings suggest this retinal-modified SELP with efficient light-induced processes could be further studied for self-assembly, drug delivery, and biomedical applications.

ASSOCIATED CONTENT

Supporting Information

Experimental details. This material is available free of charge via the Internet at <http://pubs.acs.org>.

AUTHOR INFORMATION

Corresponding Author

David.Kaplan@tufts.edu

Notes

The authors declare no competing financial interest.

ACKNOWLEDGMENTS

Support from the NIH EB014283 and EB002520 is gratefully acknowledged, as is support from the Air Force Office of Scientific Research.

REFERENCES

- Omenetto, F. G.; Kaplan, D. L. *Science* **2010**, *329*, 528.
- Vasconcelos, A.; Gomes, A. C.; Cavaco-Paulo, A. *Acta Biomater.* **2012**, *8*, 3049.
- Bracalello, A.; Santopietro, V.; Vassalli, M.; Marletta, G.; Del Gaudio, R.; Bochicchio, B.; Pepe, A. *Biomacromolecules* **2011**, *12*, 2957.
- An, B.; Desrochers, T. M.; Qin, G.; Xia, X.; Thiagarajan, G.; Brodsky, B.; Kaplan, D. L. *Biomaterials* **2013**, *34*, 402.
- Qin, G.; Hu, X.; Cebe, P.; Kaplan, D. L. *Nat. Commun.* **2012**, *3*, 1003.
- Chow, D.; Nunalee, M. L.; Lim, D. W.; Simnick, A. J.; Chilkoti, A. *Mater. Sci. Eng., R* **2008**, *62*, 125.
- Xia, X. X.; Xu, Q.; Hu, X.; Qin, G.; Kaplan, D. L. *Biomacromolecules* **2011**, *12*, 3844.
- Qiu, W.; Cappello, J.; Wu, X. *Appl. Phys. Lett.* **2011**, *98*, 263702.
- Chang, J.; Peng, X. F.; Hijji, K.; Cappello, J.; Ghandehari, H.; Solares, S. D.; Seog, J. *J. Am. Chem. Soc.* **2011**, *133*, 1745.
- Qiu, W.; Huang, Y.; Teng, W.; Cohn, C. M.; Cappello, J.; Wu, X. *Biomacromolecules* **2010**, *11*, 3219.
- Gustafson, J. A.; Price, R. A.; Greish, K.; Cappello, J.; Ghandehari, H. *Mol. Pharmaceutics* **2010**, *7*, 1050.

- (12) Greish, K.; Araki, K.; Li, D.; O'Malley, B. W., Jr.; Dandu, R.; Frandsen, J.; Cappello, J.; Ghandehari, H. *Biomacromolecules* **2009**, *10*, 2183.
- (13) Haider, M.; Leung, V.; Ferrari, F.; Crissman, J.; Powell, J.; Cappello, J.; Ghandehari, H. *Mol. Pharmaceutics* **2005**, *2*, 139.
- (14) Megeed, Z.; Cappello, J.; Ghandehari, H. *Adv. Drug Delivery Rev.* **2002**, *54*, 1075.
- (15) Alonso, M.; Reboto, V.; Guiscardo, L.; Mate, V.; Rodriguez-Cabello, J. C. *Macromolecules* **2001**, *34*, 8072.
- (16) Cronin-Golomb, M.; Murphy, A. R.; Mondia, J. P.; Kaplan, D. L.; Omenetto, F. G. *J. Polym. Sci., Part B: Polym. Phys.* **2012**, *50*, 257.
- (17) Sovdat, T.; Bassolino, G.; Liebel, M.; Schnedermann, C.; Fletcher, S. P.; Kukura, P. *J. Am. Chem. Soc.* **2012**, *134*, 8318.
- (18) Wu, P. F.; Bhamidipati, M.; Coles, M.; Rao, D. V. G. L. N. *Chem. Phys. Lett.* **2004**, *400*, 506.
- (19) Han, M.; Smith, S. O. *Biochemistry* **1995**, *34*, 1425.
- (20) Asakura, T.; Nishi, H.; Nagano, A.; Yoshida, A.; Nakazawa, Y.; Kamiya, M.; Demura, M. *Biomacromolecules* **2011**, *12*, 3910.
- (21) Creager, M. S.; Izdebski, T.; Brooks, A. E.; Lewis, R. V. *Comp. Biochem. Physiol., Part A: Mol. Integr. Physiol.* **2011**, *159*, 219.
- (22) Omenetto, F.; Kaplan, D. *Sci. Am.* **2010**, 303, 76.
- (23) Tao, H.; Chieffo, L. R.; Brenckle, M. A.; Siebert, S. M.; Liu, M.; Strikwerda, A. C.; Fan, K.; Kaplan, D. L.; Zhang, X.; Averitt, R. D.; Omenetto, F. G. *Adv. Mater.* **2011**, *23*, 3197.
- (24) Tao, H.; Kaplan, D. L.; Omenetto, F. G. *Adv. Mater.* **2012**, *24*, 2824.
- (25) Tao, H.; Amsden, J. J.; Strikwerda, A. C.; Fan, K.; Kaplan, D. L.; Zhang, X.; Averitt, R. D.; Omenetto, F. G. *Adv. Mater.* **2010**, *22*, 3527.
- (26) Tao, H.; Brenckle, M. A.; Yang, M.; Zhang, J.; Liu, M.; Siebert, S. M.; Averitt, R. D.; Mannoor, M. S.; McAlpine, M. C.; Rogers, J. A.; Kaplan, D. L.; Omenetto, F. G. *Adv. Mater.* **2012**, *24*, 1067.
- (27) Omenetto, F. G.; Kaplan, D. L. *Biomaterials* **2010**, *31*, 6119.
- (28) Omenetto, F. G.; Kaplan, D. L. *Nat. Mater.* **2012**, *11*, 273.